Network Office (University of Washington, Seattle, WA, 1996).
24. G. G. McGee, D. J. Leopold, R. D. Nyland, *Ecol. Appl.* **9**, 1316 (1999).
25. D. R. Foster *et al.*, *BioScience* **47**, 437 (1997).
26. J.C. Jenkins, R.A. Birdsey, Y. Pan, *Ecol. Appl.* **11**, 1174 (2001).
27. R. H. Whittaker, F. H. Bormann, G. E. Likens, T. G. Siccama, *Ecol. Monogr.* **44**, 233 (1974).
28. In 1998 to 2000, AGWI was 1.1, 1.2, and 1.4 Mg C ha^{-1} $year^{-1}$, respectively.
29. I. L. Sander, in R. M. Burns, B. H. Honkala, Eds., *Silvics of North America* (Agriculture Handbook 654, Forest Service/U.S. Department of Agriculture, Washington, DC, 1990).
30. J. D. Aber *et al.*, *BioScience* **48**, 921 (1998).
31. P. S. Curtis, X. Z. Wang, *Oecologia* **113**, 299 (1998).
32. J. W. Munger *et al.*, *J. Geophys. Res.* **103** (D7), 8355 (1998).
33. Supplementary Web material is available on *Science* Online at www.sciencemag.org/cgi/content/full/294/5547/1688/DC1.
34. K. E. Savage, E. A. Davidson, *Global Biogeochem. Cycles* **15**, 337 (2001).
35. It is unlikely that variation in leaf litter fall contributed significantly to variation in heterotrophic respiration, because annual litter fall in our study was quite consistent (e.g., 1.30 and 1.37 Mg C ha^{-1} in 1998 and 1999, respectively).
36. See www.lternet.edu/hfr/symposium/symp01/symp01abs.html#davidson
37. T. T. Kozlowski, *Bot. Rev.* **58**, 107 (1992).
38. The daily average NEE at Harvard Forest normally becomes negative in late May (*16*). This roughly coincides with the date that new leaves begin to export C to the trees (>50% leaf expansion) (*37*). See Harvard Forest phenology data at www.lternet.edu/hfr/data/hf003/hf003.html.
39. Annual variation in tree mortality did not contribute directly to uncertainty in the biometric C budget (see Table 1), but did add uncertainty to the estimate of the mean CWD respiration rate. To find this rate, we began with the current (year 2000) measured stock of aboveground CWD (7.5 Mg C ha^{-1}; composed of 5.5 Mg C ha^{-1} standing snags and 2.0 Mg C ha^{-1} logs). We then calculated the aboveground CWD present midway through the study, assuming constant tree mortality (mean mortality for 1993 to 2000 = 0.64 Mg C ha^{-1} $year^{-1}$ aboveground). We assumed dead woody roots = 20% of aboveground CWD (*27*). We then calculated 6% annual loss of C (*40*) from the total time-averaged CWD pool. The confidence interval for CWD respiration (and thus for ΔCWD) reflects only the statistical uncertainty in the CWD pool size. There was no statistical basis for estimating the uncertainty associated with our choice of 6% annual respiration of CWD, and therefore we omitted it from the overall budget. Thus, it is possible that the confidence interval about the estimate of NEP should be slightly larger. However, we believe that the central estimate is conservative because the majority of standing snags in the CWD pool argues against rapid CWD decomposition.
40. D. P. Turner, G. J. Koerper, M. E.Harmon, J. J. Lee, *Ecol. Appl.* **5**, 421 (1995).
41. R. A. Birdsey, A. J. Plantinga, L. S. Heath, *For. Ecol. Manage.* **58**, 33 (1993).
42. P. E. Kauppi, K. Mielikäinen, K. Kuusela, *Science* **256**, 70 (1992).
43. R. N. Sampson, D. Hair, Eds., *Forests and Global Change*, vol. 2, *Forest Management Opportunities for Mitigating Carbon Emissions* (American Forests, Washington DC, 1996).
44. J. B. Gaudinski, S. E. Trumbore, E. A. Davidson, S. Zheng, *Biogeochemistry* **51**, 33 (2000).
45. We thank J. Budney, B. Daube, A. Bright, K. Bagstad, F. Frizzell, S. Heath, and D. Patterson for technical assistance. This work was supported by grants from the U.S. Department of Energy (DE-FG02-95ER62002, NIGEC DE-FC03-90ER61010), National Science Foundation (ATM-99-81782, DEB-008-0592, BSR-88-11764), National Aeronautics and Space Administration (NAGW-3082), and Harvard University (Division of Engineering and Applied Science and the Harvard Forest).

30 May 2001; accepted 23 October 2001

A Near-Earth Asteroid Population Estimate from the LINEAR Survey

Joseph Scott Stuart

I estimate the size and shape of the near-Earth asteroid (NEA) population using survey data from the Lincoln Near-Earth Asteroid Research (LINEAR) project, covering 375,000 square degrees of sky and including more than 1300 NEA detections. A simulation of detection probabilities for different values of orbital parameters and sizes combined with the detection statistics in a Bayesian framework provides a correction for observational bias and yields the NEA population distribution as a function of absolute magnitude, semi-major axis, eccentricity, and inclination. The NEA population is more highly inclined than previously estimated, and the total number of kilometer-sized NEAs is 1227^{+170}_{-90} (1σ).

Attempts to estimate the number of NEAs (*1*) have always been hampered by selection biases inherent to all observations as well as by small detection sample sizes. Bottke *et al.* (*2*, *3*) addressed this problem by using theoretical orbital dynamical constraints in combination with 138 detections from the SPACEWATCH program to constrain the size and shape of the NEA population. Rabinowitz *et al.* (*4*) estimated the NEA population using 45 detections from the NEAT program. Here, I use the order-of-magnitude larger detection sample size of the LINEAR project (*5*) to estimate the size and shape of the NEA population constrained solely by observational data. An estimate of the number of NEAs as a function of absolute magnitude, which is related to the size of the asteroid, is of critical importance in assessing the collision hazard for Earth. The distribution of the orbital parameters of the NEAs is important for understanding processes of solar system formation and dynamics and for evaluating the collision hazard.

In 3 years of operation, the LINEAR project searched almost 500,000 square degrees (*6*) of sky on nearly 600 nights, discovering 657 new NEAs and over 110,000 new main-belt asteroids. On many of the nights, however, the weather was sufficiently variable that it was difficult to characterize the limiting magnitude of the search. Selecting only the nights with stable atmospheric transparency leaves 412 nights, covers more than 375,000 square degrees of sky, and includes 1343 detections of 606 different near-Earth asteroids (Fig. 1).

To understand the selection biases of the LINEAR system, one must know where the telescope searched each night, the nightly brightness threshold for detecting an NEA, and the identities of all NEAs detected. The nightly observing logs provide the search locations and areas to within a few arcseconds. Determining the nightly brightness threshold is more difficult. Because of LINEAR's short integration times (*7*) and large pixels (2.2 by 2.2 arcseconds), NEAs move less than the size of a pixel. Asteroids and stars are all point sources, thus they can be treated with the same photometric model. The 50% detectability threshold is established using the signal-to-noise ratios of 200 to 300 cataloged solar-type stars in each field. The limiting magnitude for each night is then set by averaging these detectability thresholds. Uncertainty in the overall bias of the limiting magnitude calculation contributes to the error estimate in the derived number of NEAs. An estimate of this error is added in quadrature with the formal statistical errors described below to obtain the final error value for the number of NEAs and the error envelopes for the distributions.

To determine which NEAs were detected on any given night, the nightly telescope logs are combined with definitive identifications provided by the International Astronomical Union's Minor Planet Center (MPC). LINEAR reports all of its observations to the MPC, including those that have motions characteristic of main-belt asteroids, and provides intentional coverage overlap after a few nights or during the following month. This follow-up allows NEAs with motions initially mimicking main-belt asteroids to be identified, so that the number of detections not identified as NEAs is low, on the order of 1% of the number of NEA detections. Errors in which main-belt asteroids or false detections are erroneously labeled as NEAs are low because all NEA detections are verified on multiple nights, and usually by multiple observers, before orbits are issued by the MPC.

To determine correction factors for observational bias in the LINEAR search, I accounted for the time-correlated nature of the asteroid search space. I divided the orbital parameter space (a-e-i-H) into 49,200 bins (*8*). In each bin, I generated 144,000 asteroid orbits (*9*). Each of these 144,000 test particles is propagated through the time covered by the search and

Massachusetts Institute of Technology Lincoln Laboratory, 244 Wood Street, Room S4-571, Lexington, MA 02421, USA. E-mail: stuart@ll.mit.edu

checked against each night's telescope pointing history. The apparent visual magnitude of each test particle is calculated from its orbital parameters and the absolute magnitude of its bin (with a photometric phase slope parameter G = 0.15). Whenever the propagated position of the test particle falls within the telescope's field of view and the calculated apparent visual magnitude of the test particle is brighter than the limiting visual magnitude of the telescope for that night, the test particle is labeled as detected by the search. After propagating all 144,000 test particles through the 3 years of the search history, the test particles that had been detected are labeled. The fraction of detected test particles relative to the total number in a bin is the observational bias of the survey for that specific a-e-i-H bin. This observational bias for an individual bin is the probability that an actual asteroid with the properties of the bin would have been detected by the survey. These detection probabilities for the 49,200 a-e-i-H bins provide a four-dimensional map of the observational bias of the LINEAR search. Using substantially fewer bins would mean applying unreasonable correction factors to detections far from a bin center.

During the nights used for this study, the LINEAR system detected 606 distinct NEAs among 1343 total NEA detections (some NEAs were detected multiple times). I divided the 606 NEAs into the 49,200 a-e-i-H bins. For each bin, I estimate N, the true number of objects in that bin. Using a binomial statistical model with N asteroids, and detection probability, p, the probability distribution for the expected number of detections, x, is a binomial distribution. The quantity x/p, where x is the observed number of detections in the bin, is an unbiased estimator for the number of asteroids in the bin. The variance of this estimator, given the true value of N, is N/p − N. To obtain errors for these estimates, one needs the variance of the true parameter value given the observed value of the estimator. This inversion is performed by applying Bayes' law in each a-e-i-H bin. The prior distributions for values of N are Gaussian with the mean and variance for each bin increasing as a power law in the H dimension and uniform in the other three dimensions.

With an unbiased estimate of the number of NEAs in each a-e-i-H bin, I could, in principle, provide a full four-dimensional map of the asteroid population. However, because there are more bins than asteroids, the number of detections in any given bin is small (either 0 or 1 in almost all cases), so the noise in the estimates for individual bins is large. However, by summing over any three of the dimensions, I obtain an estimate of the distribution over the fourth parameter with robust statistics (no fewer than 20 detections per one-dimensional bin).

The predicted size of the NEA distribution (Fig. 2) with $H < 18$ (*10*) is 1227^{+170}_{-90} (1σ). My estimate of the number of NEAs with $H < 18$ is higher than the recent measurement by Rabinowitz *et al.* (750 ± 150) (*4*). The Rabinowitz model, limited by the small number of NEA detections in that survey, was unable to independently estimate the distributions over a, e, and i, and thus made assumptions about the distributions of the orbital parameters. Those assumptions may account for the discrepancy between the two estimates. Bottke *et al.* (*2*, *3*) recently estimated the number of $H < 18$ NEAs as 910^{+100}_{-120}. The shape of my population estimate over inclination differs from the Bottke model. This difference probably accounts for the difference in the overall size of the population estimates. These results assume uniformly distributed values for argument of perihelion, longitude of the ascending node, and mean anomaly. If this assumption is invalid, the true population is likely to be larger than estimated here.

The orbital parameter distributions (Fig. 3) are similar to those obtained by Bottke *et al.* using theoretical dynamical constraints on the orbital distributions of NEAs. The models differ primarily in the inclination distribution. This estimate indicates more high-inclination NEAs in comparison to Bottke's model. Bottke's four-dimensional theoretical model has substantial coupling between the semi-major axis distribution and the inclination distribution. In that model, NEAs with semi-major axes less than 1.8 astronomical units (AU) have higher inclinations than NEAs with semi-major axes beyond 2 AU. The discrepancy between Bottke's inclination distribution and mine is unlikely to be caused by this coupling between the semi-major axes and inclinations of the NEAs. The LINEAR search data used here has 244 detections beyond 2 AU, and the bias correction method used here does not force an assumed semi-major axis distribution to obtain the inclination distribution. The semi-major axis distribution (Fig. 3) matches that estimated by Bottke *et al.*, as does the eccentricity distribution. The small shift toward lower eccentricities may be explained by a binning effect. If the shape of the real NEA inclination distribution ultimately matches the model presented here, it may imply a slightly different ratio of contributions from main-belt source regions than the contributions derived by Bottke *et al.* The similarity between these results and those of Bottke *et al.* represents a convergence between NEA observation and theoretical modeling of solar system dynamics.

This estimate of the size of the NEA population (Fig. 2) is higher than recent estimates and is closer to previous estimates by Shoemaker *et al.* (*11*). The size of the NEA population is an important component in assessing the long-

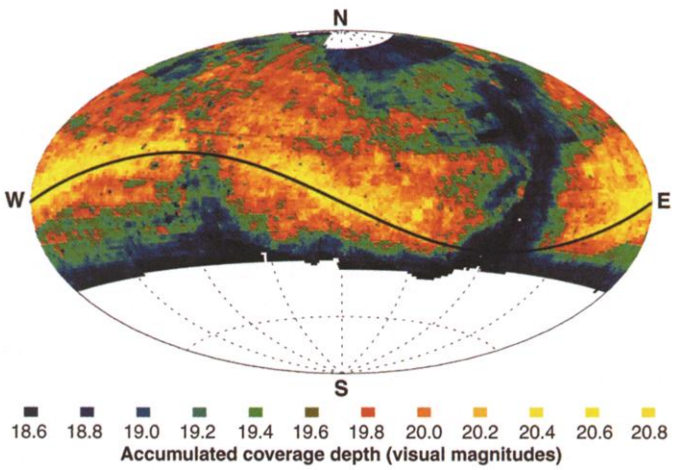

Fig. 1. An equal-area projection of the entire celestial sphere in right ascension and declination coordinates showing the area coverage and accumulated depth of the LINEAR survey data used in this analysis. The ecliptic plane is plotted in black for reference. Nearly 2 million square degrees of sky imaging (*6*) are represented based on surveying conducted from March 1998 through February 2001. The color-coded accumulated depth is the equivalent limiting magnitude from combining multiple searches of each field.

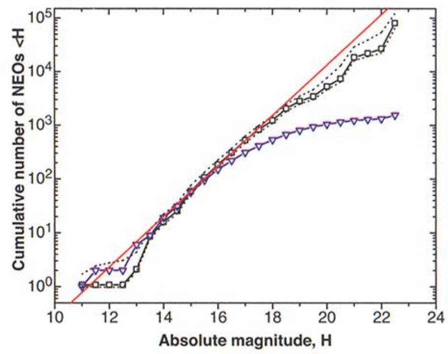

Fig. 2. Cumulative H magnitude distribution of the NEA population. The black squares are my estimate of the population, with 1σ error envelope (dotted lines). The known population (as of 9 October 2001) is shown as blue triangles. The number of NEAs with $H < 18$ is 1227^{+170}_{-90} (1σ). The red line indicates the best straight line fit to the middle portion ($14 < H < 18.5$) of the H distribution. I fit a straight line to the logarithm (base 10) of the noncumulative H distribution with bin size of 0.5. The noncumulative best-fit line is $N(H) = 10^{-4.33+0.39H}$. The fit for the offset is −4.33 ± 0.22 and for the slope is 0.39 ± 0.013. Translating the noncumulative fit to a cumulative distribution yields a fit of $N(<H) = 10^{-3.88+0.39H}$.

term probability of collision between NEAs and Earth. The risk of collision between NEAs and Earth is partially offset by the fact that the NEAs have higher inclinations than previously thought, because NEAs with higher inclinations are less likely to impact the Earth (*12*). The size and shape of the NEA population is important for understanding the collision hazard for Earth, and their availability for study by space missions and for utilization as space resources. The distribution of NEA inclinations could provide insight into where the NEAs formed and how they move through the solar system.

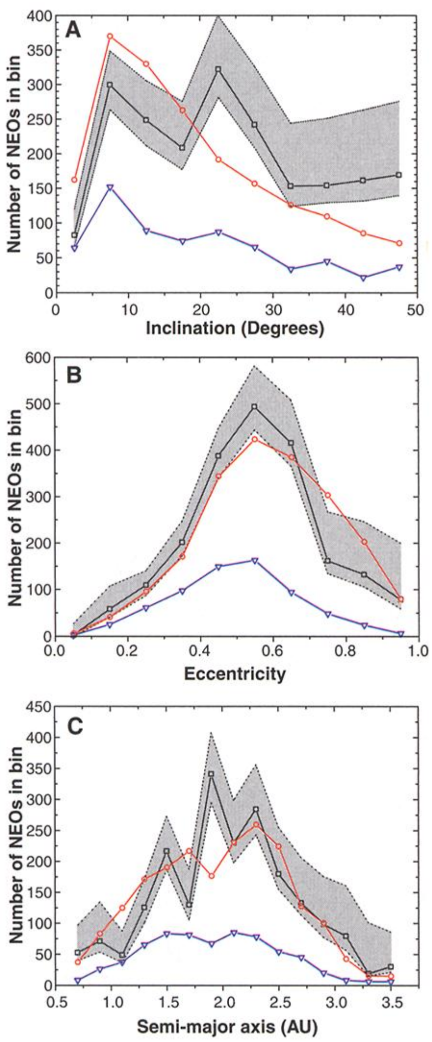

Fig. 3. Estimated distributions of the NEAs over the three orbital parameters: inclination (**A**), eccentricity (**B**), and semi-major axis (**C**). Each plot shows my estimate (black squares) of the population distribution with 1σ error bars (dotted lines and gray shading). Plotted for reference are the known NEAs (blue triangles) as of 9 October 2001 and the estimate recently published by Bottke *et al.* (*3*) (red circles). For comparison purposes, the curves from Bottke's model have been rescaled so that the total number of objects in the Bottke curves is the same as the total number of objects in the estimate given here. These curves include the estimates for the NEAs with $H < 18.5$ rather than $H < 18$ because the greatest number of detections used in this analysis fell within the $18.0 < H < 18.5$ bin. The spikes in the semi-major axis distribution are probably random fluctuation because they are consistent with the error envelope. The spikes in the inclination distribution are probably real because they appear in the known distribution.

References and Notes

1. The term near-Earth asteroids (NEAs) refers to asteroids with perihelia less than 1.3 AU, and aphelia greater 0.983 AU. This definition does not include objects with observable cometary comas or tails, although cataloged asteroids may include extinct comet nuclei.
2. W. F. Bottke, R. Jedike, A. Morbidelli, J. Petit, B. Gladman, *Science* **288**, 2190 (2000).
3. W. F. Bottke *et al.*, *Icarus*, in press.
4. D. Rabinowitz, E. Helin, K. Lawrence, S. Pravdo, *Nature* **403**, 165 (2000).
5. G. Stokes, J. Evans, H. Viggh, F. Shelly, E. Pearce, *Icarus* **148**, 21 (2000).
6. The LINEAR detection algorithm images each telescope field five times per night at half-hour intervals. Thus, 500,000 square degrees of coverage represents 2.5 million square degrees of imaging.
7. The integration times in this survey were selected to allow the system to cover 600 fields (about 1200 square degrees) while filling up the time available during the night. In winter, this allows for 11-s integration times, whereas in summer, as little as 3 s.
8. The a-e-i-H parameter space is broken into bins that are 0.1 AU wide in semi-major axis, 0.1 wide in eccentricity, 5° wide in inclination, and 0.5 magnitudes wide in absolute magnitude. For the plot in Fig. 3, the semi-major axis dimension was converted to bins 0.2 AU wide. The ranges of the parameters are 0.6 to 3.6 AU in semi-major axis, 0 to 1 in eccentricity, 0 to 50° in inclination, and 11 to 23 magnitudes in absolute magnitude. Bins with a-e values that do not meet the definition of NEA (*1*) are excluded.
9. The arguments of perihelion and the longitudes of the ascending node are assigned by a pseudo-random number generator producing a uniform distribution from 0° to 360°. The mean anomalies are evenly spaced from 0° to 360° at intervals of 0.5°.
10. I use the convention that absolute magnitude H = 18 corresponds to a diameter of 1 km. Absolute magnitude is the apparent brightness an object would have if placed at a theoretical position 1 AU from Earth and 1 AU from the Sun, with a Sun-asteroid-Earth phase angle of zero degrees. The correspondence of H = 18 with a diameter of 1 km is equivalent to using an albedo of 0.11, a widely assumed average value.
11. E. M. Shoemaker, R. F. Wolfe, C.S. Shoemaker, *Geol. Soc. Am. Spec. Paper 247* (1990), pp. 155–170.
12. E. J. Öpik, *Proc. R. Irish Acad.* **54A**,165 (1951).
13. Sponsored by the Department of the Air Force and NASA under Air Force Contract F19628-00-C-0002. Opinions, interpretations, conclusions, and recommendations are those of the author and are not necessarily endorsed by the United States Air Force. The author acknowledges financial support from the Lincoln Scholars Program at MIT Lincoln Laboratory. The author wishes to thank R. Binzel for guidance, F. Shelly and the telescope operators for collecting the data used in this analysis, and P. Hopman and R. Sayer for technical advice.

13 August 2001; accepted 12 October 2001

Dynamical Spreading of Asteroid Families by the Yarkovsky Effect

William F. Bottke Jr.,[1] David Vokrouhlický,[2] Miroslav Brož,[2] David Nesvorný,[1] Alessandro Morbidelli[3]

The orbital distributions of prominent asteroid families are thought to be direct by-products of catastrophic disruption events among diameter $D \gtrsim 100$ kilometer bodies. Ejection velocities derived from studying observed families, however, are surprisingly high compared with results from impact experiments and simulations. One way to resolve this apparent contradiction is by assuming that $D \lesssim 20$ kilometer family members, since their formation, have undergone semimajor axis drift by the thermal force called the Yarkovsky effect. Interactions between drifting family members and resonances can also produce unique eccentricity and/or inclination changes. Together, these outcomes help explain (i) why families are sharply bounded by nearby Kirkwood gaps, (ii) why some families have asymmetric shapes, and (iii) the curious presence of family members on short-lived orbits.

Catastrophic collisions among large asteroids in the main belt are believed to produce asteroid families [e.g., (*1*)]; clusters of asteroid fragments with similar proper semimajor axes *a*, eccentricities *e*, and inclinations *i* (*2*, *3*); and spectral signatures consistent with an origin from a common parent body (*4*, *5*). As such, prominent asteroid families (e.g., Koronis, Eos, Themis, Eunomia, and Vesta) are natural laboratories for understanding high-velocity impact physics, one of the principal geologic processes affecting small bodies in the solar system.

Although this formation scenario is straightforward, there are still many aspects of asteroid families that we do not yet under-

[1]Southwest Research Institute, 1050 Walnut Street, Suite 426, Boulder, CO 80302, USA. [2]Institute of Astronomy, Charles University, Prague, V Holešovičkách 2, 180 00 Prague 8, Czech Republic. [3]Observatoire de la Côte d'Azur, B.P. 4229, 06034 Nice Cedex 4, France.

*To whom correspondence should be addressed. E-mail: bottke@boulder.swri.edu